e-ISSN No.: 2582-4228

Journal of Indian Association for Environmental Management

Journal homepage: www.http://op.niscair.res.in/index/php/JIAEM/index

Highly Efficient Capture of Reactive Orange 16 Dye from Industrial Wastewater using Sodium Tripolyphosphate Crosslinked Chitosan-charcoal Composite

P. M. Nandanwar[a]*, R. M. Jugade[a]

Department of Chemistry, RTM Nagpur University, Nagpur, India-440033
*Corresponding author: Email: pradipnandanwar27@gmail.com

Submitted: 22 July 2024 Revised: 03 September 2024 Accepted: 05 September 2024

***Abstract*: In this study, we developed a chitosan-charcoal composite (Cs–Ac) crosslinked with sodium tripolyphosphate (STPP) for the efficient removal of Reactive Orange 16 dye from aqueous solutions. The Cs–Ac composite was thoroughly characterized using Fourier transform infrared spectroscopy (FTIR), X-ray diffraction (XRD), scanning electron microscopy (SEM), energy dispersive X-ray spectroscopy (EDX), and pH point of zero charge (pH_pzc) analysis to understand its physicochemical, structural, and morphological properties. The material was subjected to the adsorption of Reactive Orange 16 dye. The effects of the solution pH, adsorbent dose, contact time, temperature, and dye concentration were examined. The equilibrium data was described well by the Langmuir isotherm model with a coefficient of determination (R^2) value of 0.9881. At near-neutral pH, with a contact time of only 60 min at room temperature, the material showed an adsorption capacity of 39.43 mg g^{-1} which is much higher in contrast to all the previously reported materials. The adsorption performance of Cs–Ac for Reactive Orange 16 dye was evaluated by examining the effects of solution pH, adsorbent dose, contact time, temperature, and dye concentration. The equilibrium data were best described by the Langmuir isotherm model, indicating monolayer adsorption with a high coefficient of determination (R^2 = 0.9881). At near-neutral pH and a contact time of 60 minutes at room temperature, the Cs–Ac composite demonstrated an impressive adsorption capacity of 39.43 mg g^{-1}, significantly outperforming previously reported materials. The kinetics of uptake was well-defined by the pseudo-second-order model chemisorption model. Evaluation of the thermodynamic parameters revealed the spontaneous, endothermic and entropy-driven nature of adsorption. Cs–Ac exhibited excellent performance in capturing Reactive Orange 16 dye from aqueous solutions. Its high adsorption capacity, coupled with favorable kinetic and thermodynamic properties, makes it a promising material for water purification applications. Further studies could explore the regeneration and reuse of the composite, as well as its effectiveness in removing other pollutants from water**

***Keywords*: Adsorption, Reactive Orange 16 dye, Chitosan, Spontaneous, Endothermic**

I. INTRODUCTION

Water is an indispensable aspect of all lives on earth, it defines the characteristic of human beings. With a very limited availability of pure water on earth, regrettably the rapid increase in water pollution is posing a challenge due to industrial and anthropogenic adulteration in water bodies (Rojas, S. et. al. 2020). The main toxicants include dyes (Naushad, M. et. al. 2019), pesticides (Ali, I. et. al. 2019), colouring matter (Wabaidur, S. M. et. al. 2020) and oils (Khan, M. et. al. 2020). Among the various distresses, textile industries are the major contributors towards the environmental pollution due to the discharge of various dyes in water bodies (Tang, H. et. al. 2012). The dyeing industry waste is one of the major concerns of the textile industry, including coloured waste water, which causes hazardous effects on the environment. Mainstream of these dyes have a complex aromatic molecular structure, and are water soluble, non-biodegradable, and toxic in nature; therefore, it has become highly vital to remove these dyes from water effluents to make the environment safe and clean in terms of shielding the livelihoods of all creatures (San Miguel, G. et. al. 2006). Reactive dyes are used for dyeing cellulosic fibres in textile industries to a large extent, and these are usually characterized by azo bonds. The colour of azo dyes is due to a

chromophoric effect of the azo group. First, the dyes are treated with cellulose and then are made to interact with the fibrous material of the cellulose (Al-Degs, Y. et. al. 2000). The reaction occurs by the formation of a covalent bond between the dye molecule and the fibre. Adsorption, electrochemical oxidation, biological treatment, coagulation, physicochemical flocculation, precipitation, ozonation, and other ample technologies have been applied and critically studied recently (Behera, M. et. al. 2021). Orthodox wastewater treatment methods have a low removal efficiency (Robinson, T. et. al. 2001). The adsorption process was found to be one of the effective techniques among several chemical, bacteriological, catalytic, and physical methods that have been successfully employed for the removal of colours from waste water due to its low cost, ease of operation, greater efficiency, and non-generation of toxic materials (Li, Z. et. al. 2019). Numerous adsorbents have been tested for their applicability in dye adsorption from effluents, such as activated sludge (Pala, A. et. al. 2002), alum (Dwyer, J. et. al. 2009), coal ash (Butt, M. T. et. al. 2010), silicates (Sun, Z. et. a. 2018), acetyl acetone (Yang, F. et. al. 2021) and graphene based nanomaterials (Faysal Hossain, M. D. et. al. 2020). The ability of chitosan to eradicate pollutants from effluents is highly appreciated due to its assorted functionality, including amino and hydroxyl functional groups in the molecule for forming various interactions, including hydrogen bonding, electrostatic interaction, and van der Waals forces of attraction (Zhou, Y. et. al. 2019). However, the insufficient strength and stability in acidic medium hamper the superior application of chitosan (Elsabee, M. Z. et. al. 2009). In order to decide these issues and to improve the physicochemical properties of chitosan, its modifications using various crosslinkers as well as by composite formation with mechanically and thermally stable materials are the most obvious pathways. Composites of chitosan with activated charcoal can be applied to improve the surface structure, morphology, and surface-assimilative property of chitosan biopolymers (Guo, M. et. al. 2019). Adding a crosslinking agent boosts the chemical stability and front-runners to microstructure improvement for its improved adsorption performance (Yang, J. et. al. 2021). Several studies have been carried out on the adsorption of water pollutants using chitosan-activated charcoal composites involving the removal of dyes in the recent years (Korde, S. et. al. 2021). Recently, we reported a composite of cellulose fabricated by the co-precipitation of Fe and Al in the cellulose material for the detoxification of various reactive dyes with high adsorption capacities (Khapre, M. A. et. al. 2021). In this study, we used a hybrid approach involving crosslinking chitosan with sodium tripolyphosphate (STPP) for enhanced mechanical strength and for entrapping activated carbon through the enhanced surface area and porosity, leading to a good sorbent with outstanding confiscation capability for Reactive Orange 16 dye.

II. MATERIALS AND METHODS

Experimental

Reagents

All the chemicals and reagents used in the experiments were of analytical grade. Chitosan with a degree of deacetylation of >90% was purchased from Sisco Research Laboratory, India. Acetic acid and 25% ammonia solution were obtained from SD Fine Chemicals Ltd (India). Activated charcoal, STPP, and Reactive Orange 16 dye were acquired from Loba Chemie (India). All the chemicals were used without further purification and deionized distilled water was used throughout the studies.

Instruments

FT-IR spectra were obtained using a Bruker AlphaE spectrometer (USA) for an average of 23 scans. A Rigaku Miniflex 300 system (Tokyo, Japan) was used for the XRD analysis. The surface morphology was studied by a scanning electron microscopy (SEM) system model TESCAN VEGA 3 SBH (Czech Republic), while EDX analysis was performed by an X-ray analyzer on an Oxford INCA Energy 250 EDS system during the SEM observations. Thermal analysis was carried out using a DTG-60 simultaneous DTA/TG instrument (Shimadzu, Japan) at a scan rate of 20 °C min^{-1} and in a nitrogen flow rate of 100 mL min^{-1}. The Brunauer–Emmett–Teller surface area was estimated by the nitrogen adsorption–desorption method on a Quantachrome Nova 2200e analyzer (Florida). The estimation of dye concentration was carried out using an Equiptronics EQ-824 instrument (India) at the dye absorption maxima of 494 nm.

Synthesis of the adsorbent

Chitosan solution was prepared using a previously reported method (Jawad, A. H. et. al. 2020) by dissolving 5 g chitosan in 500 mL of 2% acetic acid. To dissolve chitosan in acetic acid, it was added gradually by keeping it under magnetic stirring for 60 min. After the complete dissolution of chitosan in acetic acid, 2.5 g activated charcoal was added step by step and the solution was kept on gentle stirring for 30 min. The resultant solution was dripped into a beaker containing 1000 mL of 6% ammonia solution with the help of a syringe, leading to the formation of spherical beads. The fresh beads were rinsed with distilled water several times for removal of all traces of ammonia. Next, 250 mL of 1% solution of STPP crosslinker was added to the beads and with very gentle stirring on a magnetic stirrer at 40 °C for 2 h. The resulting Cs–Ac beads were washed with distilled water several times and dried overnight in a hot air oven at 50 °C. The beads were crushed by a pestle and mortar and sieved to 100 micron mesh before being used in the adsorption experiments.

Batch adsorption tests

In each experiment, 25 mL dye solution of a predecided concentration along with a known weight of Cs–Ac, was stirred on a magnetic stirrer for a predetermined time. It was then filtered and the residual concentration of the solution was evaluated spectrophotometrically. Triplicate observations were obtained and the mean values were reported. The equilibrium adsorption efficiency in mg g^{-1} was calculated as (Kenawy, E. R. et. al. 2018).

$$q_e = \frac{(C_0 - C_e)V}{W}$$

Where Co (mg L^{-1}) and Ce (mg L^{-1}) are dye concentration initially and at equilibrium respectively while W (g) is the weight of adsorbent used in respective study.

Trial runs were performed to compare the adsorption efficiencies of unmodified and sequentially modified adsorbents for the Reactive Orange 16 dye. For this, 50 mg L^{-1} dye solution was equilibrated for 60 min with 100 mg of unmodified chitosan, activated charcoal, STPP crosslinked chitosan, and Cs–Ac composite in different flasks. The solution phase concentrations in each flask were determined after filtration and the adsorption efficiency was calculated for each of them.

The pHpzc of Cs–Ac was determined by a previously reported method (Kahu, S. et. al. 2016) in order to establish the surface charge on the adsorbent. For this, 50 mL 0.1 M NaCl solutions with varying initial pH from 2.0 to 9.0 were taken in a series of conical flasks. These solutions were stirred with 100 mg of Cs–Ac for 24 h. The final pH of the supernatant solutions were measured. A graph was plotted of the change in pH as a function of the initial pH, with the point it intersects the x-axis called the pH point of zero charge.

For studying the effect of the initial solution pH on the adsorption efficiency, a series of dye solutions of 100 mg L^{-1} were prepared and their pH was varied from 4.0 to 9.0. To each of the systems, 100 mg of Cs–Ac adsorbent was administered and equilibrated for 30 min. After that, the systems were filtered and the absorbance values were obtained.

The kinetics of adsorption was studied by equilibrating 100 mg L^{-1} dye solution with 25, 50, and 100 mg of Cs–Ac from 5 to 150 min. The residual solution phase dye concentration was determined after filtration.

In order to study the effect of the initial dye concentration, various dye concentrations from 20 to 400 mg L^{-1} were equilibrated with 25, 50, and 100 mg Cs–Ac for 60 min and then the dye concentration in the solution was determined.

The Cs–Ac dose was increased from 25 to 300 mg. Four dye concentrations of 50, 100, 150, and 200 mg L^{-1} were stirred with various doses of Cs–Ac for the optimized contact time of 60 min and then their final concentrations were determined spectrophotometrically.

To study the effect of temperature as part of the evaluation of the thermodynamics parameters, the temperature was varied from 298 to 333 K. The quantity of adsorption of Reactive Orange 16 upon Cs–Ac was investigated at an initial Reactive Orange 16 concentration of 100 mg L^{-1} using a 25 mL volume and adsorbent dose of 100 mg.

III. Results and Discussion

Characterization of Cs–C

Fig. 1a and 1b depicts the FT-IR spectra of Cs–Ac and Cs–Ac after Reactive Orange 16 dye adsorption. The Cs–Ac spectrum showed a characteristic broad peak around 3440 cm^{-1} corresponding to the stretching vibrations of –NH and –OH bonds in chitosan along with a skeletal vibration peak of C–O–C at 1015 cm^{-1}. (Tandekar, S. et. al. 2021). A highly intense peak at 602 cm^{-1} corresponding to O–P–O bending of the STPP group confirmed the crosslinking of chitosan with STPP. Peaks observed at 1630 and 1562 cm^{-1} could be attributed to the linkage between the phosphoric and ammonium ions. These results were attributed to the crosslinking between the amino groups of chitosan and phosphate groups of STPP (Bhumkar, D. R. et. al. 2006). After adsorption of the dye on the Cs–Ac surface, the important peaks were found to shift from their positions, indicating an interaction between the adsorbate and adsorbent molecules. The reduction in the intensity of the peak around 3440 cm^{-1} was an indication of the strong interaction between –OH and $–NH_2$ groups of chitosan with the Reactive Orange 16 molecules, consistent with the reported literature (Theerakarunwong, C. et. al. 2020).

The crosslinking could be further confirmed by EDX studies of Cs–C (Fig. 1c). The EDX spectrum showed the important peaks for phosphorous and sodium along with those of carbon and oxygen, indicating the incorporation of tripolyphosphate moieties in the chitosan framework.

XRD analysis was carried out to determine the crystalline and/or amorphous nature of Cs–Ac, as shown in Fig. 1d. (Alothman, Z. A. et. al. 2020). The diffractogram clearly showed the characteristic peaks of chitosan at 2y = 10.51 and 20.11, corresponding to the (020) and (110) planes. The slightly crystalline nature of the chitosan matrix could be attributed to the intermolecular and intramolecular hydrogen bonding. The XRD pattern of Cs–Ac showed additional peaks at 2y = 44.51 and 64.91, which were typical for the tripolyphosphate crosslinked chitosan (Qi, X. et. al. 2019).

The SEM micrographs of Cs–Ac (Fig. 1e) revealed that the surface was non-uniform and heterogeneous. This heterogeneity led to an overall enhancement in the surface area and hence in the adsorption efficiency.

The TGA curve of Cs–Ac. (Fig. 1f) showed a small weight loss of about 15% up to 150 °C associated with an endothermic crest in the DTA curve corresponding to the loss of moisture. A second major weight loss of about 50–55% occurred between 330 °C and 500 °C and was associated with an exothermic peak in the DTA curve indicating the degradation of the polymeric organic framework (Leal, G. F. et. al. 2015).

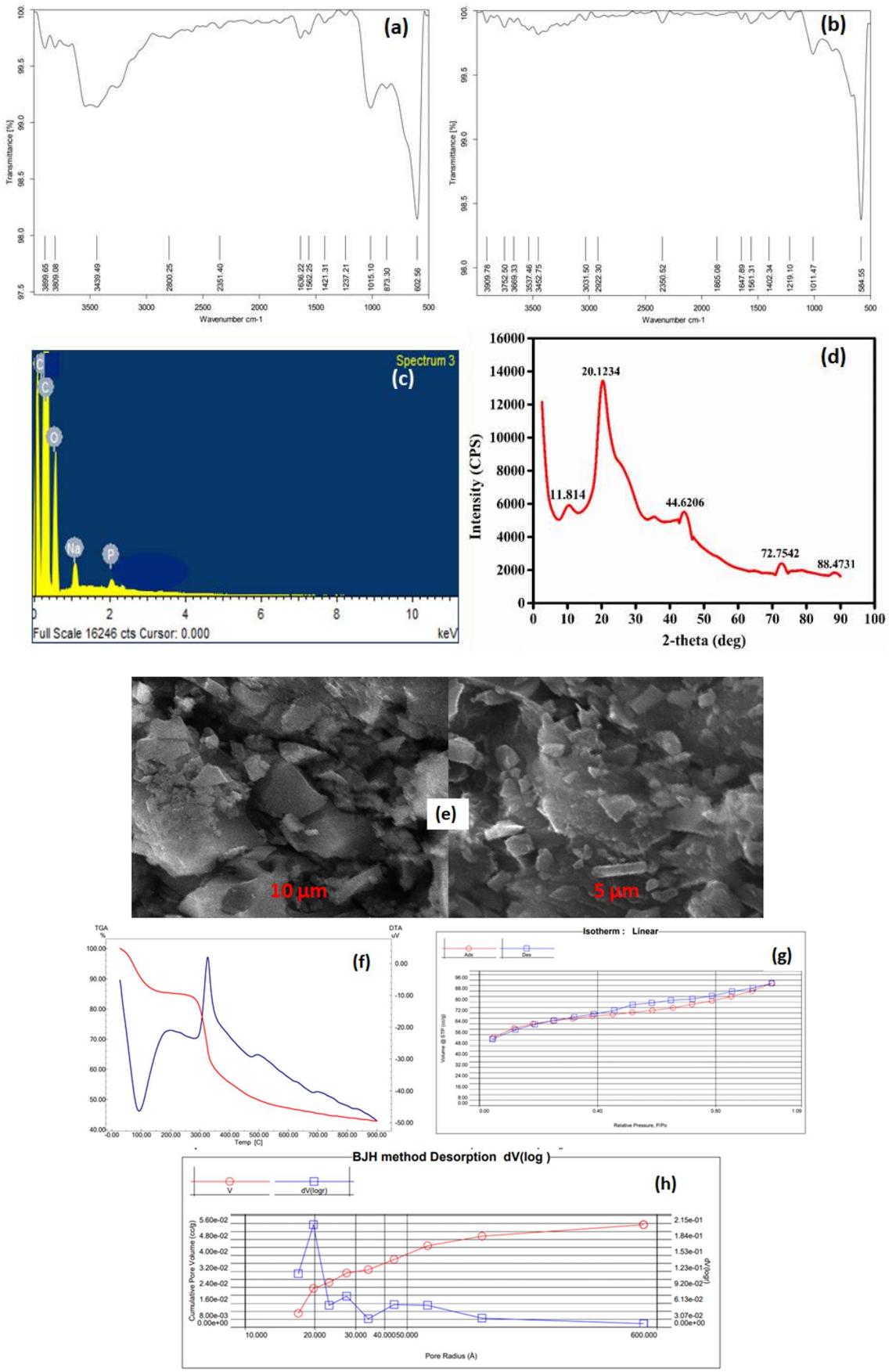

Fig. 1. (a) FT-IR spectra of Cs–Ac (a) before and (b) after the adsorption of Reactive Orange 16. (c) EDX spectrum of Cs–Ac (d) XRD spectrum, (e) SEM micrographs of Cs–Ac at two different resolutions. (f) TGA–DTA curve, (g) N_2 adsorption–desorption curves, and (h) pore-size distribution curves of Cs–Ac.

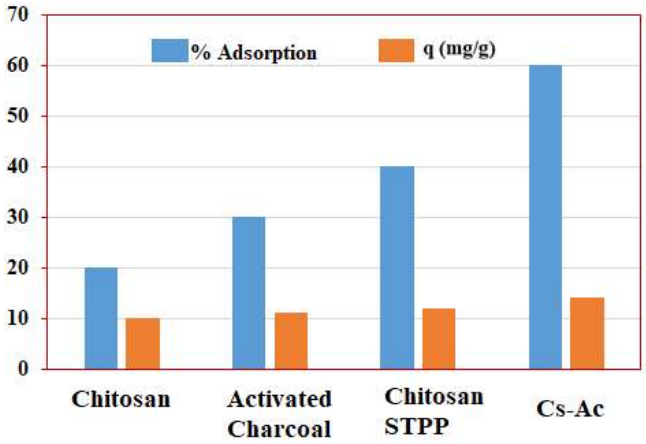

Fig. 2. Comparison of the adsorption efficiencies of various materials

The pore dimensions and surface area of Cs–Ac were determined by N_2 adsorption–desorption isotherms, as depicted in Fig. 1g, while the pore-size distribution is shown in Fig. 1g. The surface area of the unmodified chitosan was found to be 0.65 m^2 g^{-1} which was found to be enhanced to 190 m^2 g^{-1} in the Cs–Ac composite. These values were obtained by BET isotherm. As Cs–Ac was a porous material, its pore properties were established through the BJH method using the nitrogen adsorption–desorption curve. The pore volume was found to be 1.388 m^3 g^{-1}, showing the highly porous nature of the material in contrast to native chitosan, which is completely non-porous in nature. The mean pore radius of 1.459 nm was an indication of the microporous nature of the composite. As shown in Fig. 1h, the N_2 physisorption isotherm could be assigned as a type IV hysteresis on the basis of IUPAC classification. This indicated the presence of micropores in the Cs–Ac structure (Korde, S. et. al. 2020).

Activated charcoal (Ac) has a large surface area and microporous structure. The incorporation of AC in the chitosan matrix led to an enhancement of the adsorption of anionic Reactive Orange 16 dye molecules on the Cs–Ac surface because of the high diffusion of Reactive Orange 16 dye molecules through the micropores of Cs–Ac (Ahmed, M. J. et. al. 2019). The hysteresis loop (Fig. 1g) was clear evidence of the presence of micro- and mesopores in the composite material. This observation was consistent with the flake-like appearance of the surface of the material as obtained in the SEM micrographs. The shift in the desorption curve towards the left was due to the cavitation-driven desertion (Ahmed, S. et. al. 2018). The high adsorption capacity of the Cs–Ac composite towards Reactive Orange 16 could be prominently attributed to the high surface area, large pore volume, and micro- and mesoporous nature of the adsorbent.

Batch adsorption studies

During the trial experiments with unmodified chitosan, pure activated charcoal, chitosan crosslinked with STPP, and the final composite Cs–Ac, each of the materials adsorbed Reactive Orange 16 dye to a different extent. It was observed that Cs–Ac adsorbed 90 % of the dye with an adsorption efficiency of 14.84 mg g^{-1} in just 60 min, and so it was established to be the best material compared to any of the precursors (Fig. 2).

Both chitosan as well as activated charcoal had a tendency to adsorb Reactive Orange 16 dye to some extent. However, the combination of the two led to a much effective adsorption owing to the enhanced surface area of charcoal and the effective molecular interactions of chitosan. Similar results were reported by Khapre, M. et. al. 2020 for successively modified materials towards alizarin red S dye.

The effects of various variables in the adsorption experiments are presented in Fig. 3. The pH at which the surface charge on Cs–Ac was zero, i.e. the pHpzc was found to be 7.8, representing that the material exhibited a near-neutral pHpzc (Fig. 3a), meaning that the Cs–Ac surface would be distinctly positive below pH 7.8 and negative above pH 7.8. It was observed that there was no significant effect of pH on the removal efficiency of dye from pH 4 to 7 (Fig. 3b). In this pH range, the surface charge on Cs–C was positive, indicating a strong attractive interaction with the anionic dye molecules. In acidic pH, the $–NH_2$ group of chitosan was protonated as $–NH_3^+$ while the Reactive Orange 16 dye has an $–SO_3$ group, which would be responsible for the interaction in the acidic range (Ozturk, G. et. al. 2020). Strong electrostatic forces between the adsorbent and adsorbate were responsible for the high adsorption capacity of Cs–Ac towards Reactive Orange 16 dye. However, with the increase in pH above 7.8, the adsorption efficiency was found to be reduced at pH 8 and 9. This was quite obvious and could be related to the surface charge of the adsorbent. Hence, the original solution with pH 6.0 was used in all the studies.

The increase in the adsorption duration from 5 min to 150 min showed a rapid increase in adsorption in the beginning. This could be attributed to the available surface for the adsorbent molecules in the beginning. As the surface got covered with the dye, the percentage adsorption reached almost saturation in 60 min. After 60 min, there was a negligible hike in removal efficiency, and so the contact time of 60 min was considered optimum for Reactive Orange 16 dye (Fig. 3c). This was quite obvious as the maximum number of sites were available on the Cs–C surface in the beginning, but over time the sites get occupied by dye molecules, and equilibrium is reached in about 60 min (Khan, T. et. al. 2022).

The increase in Reactive Orange 16 concentration led to a reduction in the percentage adsorption but increase in the value of qe (Fig. 3d). As the concentration of incoming Reactive Orange 16 molecules increased, the relative availability of active adsorption sites decreased, thus lowering the removal percentage. However, the gathering of the excess dye on the adsorbent surface enhanced its adsorption capacity in terms of mg of dye adsorbed per gram of adsorbate material. As the adsorbent dose was increased, the availability of the surface increased and so the accumulation per unit mass (qe) went on decreasing with the increase in adsorbent dose for the same concentration. With this context, an initial dye concentration of 100 mg L^{-1} was fixed for the further studies.

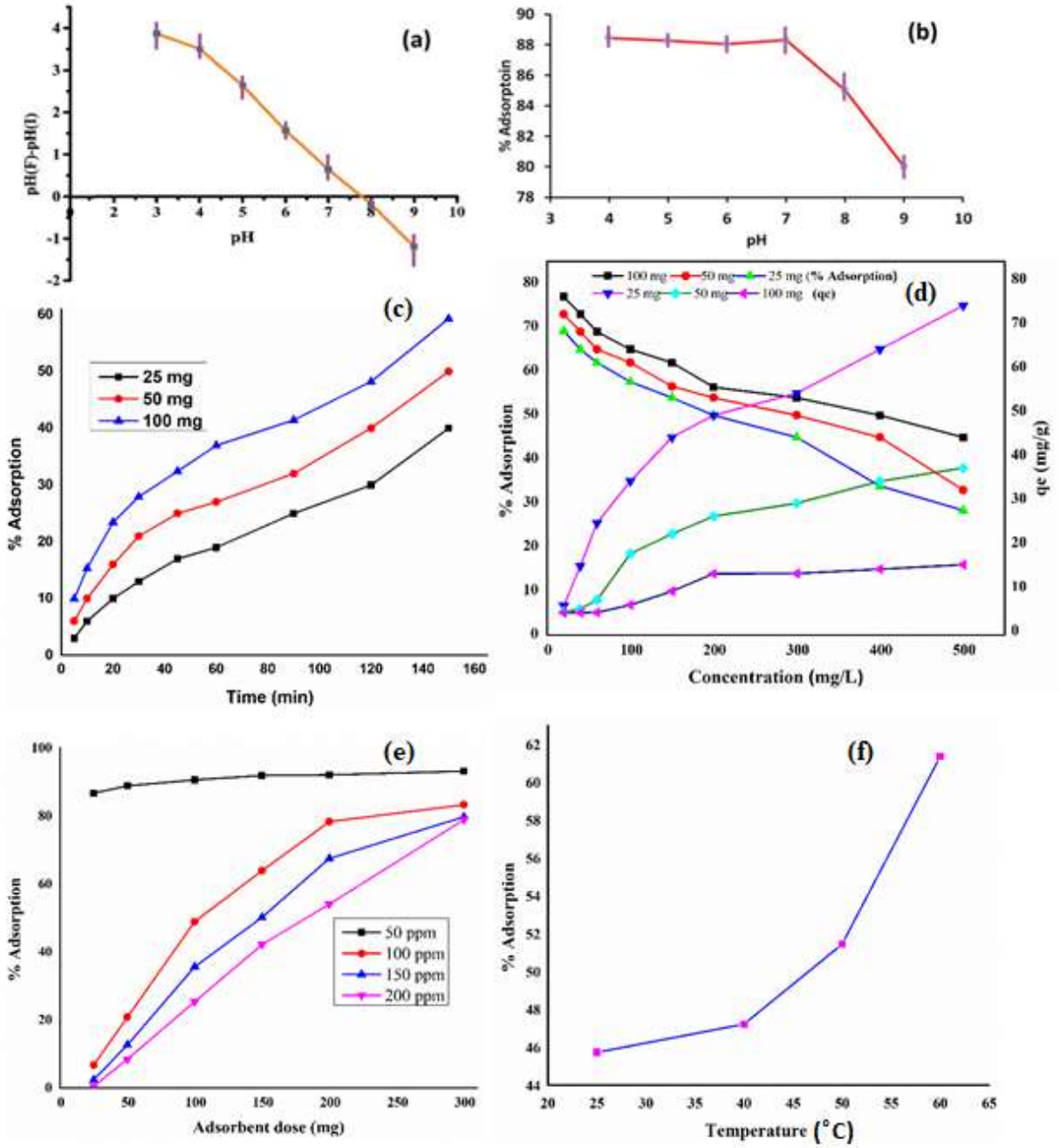

Fig. 3. (a) pHpzc of Cs–Ac. Effect of: (b) the solution pH, (c) contact time, (d) initial dye concentration, (e) adsorbent dose, and (f) temperature on the adsorption efficiency

As the Cs–Ac amount was increased from 25 mg to 300 mg, the availability of a greater number of active adsorption sites led to an enhancement in the adsorption percentage (Fig. 3e). For 100 mg L^{-1} solution, an adsorbent dose of 100 mg was found to give more than 90 % adsorption, and so this dose was selected as the optimum dose.

It was observed that the adsorption was favoured by rise in temperature, indicating the endothermic nature of the adsorption process (Fig. 3f). The simultaneous effect of two parameters is depicted in Fig. 3g and h. These graphs clearly indicate that a longer adsorption period, higher adsorbent dose, and lower dye concentration led to a greater percentage adsorption.

Isotherms, kinetics, and thermodynamics of the adsorption process

Adsorption isotherms were applied as mathematical models that could be used to predict the interaction between Reactive Orange 16 and the Cs–Ac adsorbent (Qi, X. et. al. 2019). The two isotherm models of Langmuir (Langmuir, I.1918) and Freundlich (Freundlich, H. M. 1906). were applied to investigate the equilibrium isotherms of the adsorption and for calculating the qmax. The Langmuir isotherm equation in linearized form is given by:

$$\frac{Ce}{q_e} = \frac{1}{bq_m} + \frac{Ce}{q_m}$$

Where qm (mg g^{-1}) and b (L mg^{-1}) are Langmuir isotherm coefficients, and qm represents the maximum adsorption capacity.

$$\ln q_e = \frac{1}{n} \ln Ce + \ln K_F$$

Where KF and n are Freundlich constants that indicate the adsorption capacity and adsorption intensity, respectively. A value of n between 1 and 10 indicates favourable adsorption.

TABLE 1
Reactive Orange 16 dye adsorption on Cs–Ac in terms of the kinetics, isotherm, and thermodynamics parameters

Studies	Model	Parameter			Observ-ation
Kinetics Studies	PFO	K_1 (min^{-1}) q_e cal (mg g^{-1}) q_e exp (mg g^{-1}) R^2			0.0120 -191.36 14.84 0.6423
	PSO	K_2 (mg g^{-1} min^{-1}) q_e cal (mg g^{-1}) q_e exp (mg g^{-1}) R^2			0.0023 14.27 14.84 0.956
	Intraparticle Diffusion	K_{int} (mg g^{-1} $min^{-1/2}$) Intercept (C) R^2			1.061 0.698 0.9834
	Langmuir				
Isotherm models	Freundlich	K_F (mg L^{-1}/n g^{-1} L^{-1}) n R^2			1.024 1.5824 0.9729
Thermodynamic parameters	Temperature	ΔG (kJ mol^{-1})	ΔH (kJ mol^{-1})	ΔS (J mol^{-1} K^{-1})	
	298 K 313 K 323 K 333 K	0.425 0.291 -0.154 -1.279	13.924	44.524	

It can be clearly seen from Table 1 and Fig.4 that the Langmuir model fitted best with the experimental data, with a coefficient of determination value very close to 1 indicating monolayer adsorption on the homogeneous surface of the adsorbent. The maximum monolayer adsorption capacity obtained from the Langmuir model was found to be 39.43 mg g^{-1}, which showed the excellent efficiency of the material. RL < 1 and 1<n<10 were indications of the feasible adsorption of the dye on the Cs–Ac surface.

Pseudo-first-order (PFO), pseudo-second-order (PSO), and intraparticle diffusion models were applied under optimized operating conditions. The models were applied in a timedependent study. As can be observed form Table 1 and Fig. 4, the PSO model was the best fitted model for the kinetics of adsorption. This was clear from the correlation coefficient (R^2) values. The calculated qe values from the PSO model were in agreement with experimental value of qe, thereby suggesting that the adsorption of Reactive Orange 16 dye on the Cs–Ac surface involved chemical interactions, such as electrostatic attraction between the negative charge of Reactive Orange 16 dye and positive charge available on the Cs–Ac surface (Subbaiah, M. V. et. al. 2016). The Weber Morris intraparticle diffusion model showed that the adsorption process was diffusion controlled in the beginning with a zero intercept and linear relation between q_t and $t^{1/2}$. However, with time, the process led to saturation and the boundary layer played an important role in the non-zero intercept of the graph. The overall intercept value of 11.03 indicated that the overall process was not just controlled by the diffusion (Qi, X. et. al. 2019).

The equilibrium constant K was established at different temperatures from 298 to 333 K taking the ratio of concentration of dye in the adsorbed phase to that in the solution phase. Using the equation ΔG°= -RTlnK, the corresponding values of ΔG were calculated, while the values of ΔH and ΔS were calculated from the intercept and slope of the vant Hoff plot of lnK as a function of 1/T. It was interesting to note that the adsorption process was endothermic in nature, but spontaneous over the entire temperature range and resulted in an increase in randomness. This showed the entropy-driven nature of the process (Table 1).

Probable mechanism

The activated charcoal provided the surface for the chitosan molecules to interact with the dye ions with an anionic sulphate group. Chitosan has protonated amine groups that have a strong electrostatic interaction with the anionic dye molecules. This was in accordance with the observation that increasing the pH in the basic range reduced the adsorption capacity of Cs–Ac and also as the $–NH_2$ peak was suppressed after adsorption of the dye molecules.

TABLE 2
Comparison of the adsorption capacities of Reactive Orange 16 dye by various adsorbents

Adsorbent	qm (mg/g)	References
Ethylene diamine-modified rice husk	16	(Lee, C. K. et. al. 2008)
Organofunctionalized kenyaite	33	(Royer, B. et. al. 2009)
Humin immobilized on silica	19.45	(Jesus, A. M. D. et. al.2011)
Surfactant zeolites	12.6	(Cunico, P. et. al. 2015)
Chitosan-Biopolymer-Entrapped Activated Charcoal(CCA) **Cs-Ac**	34.62 **39.43**	(Nandanwar, P. et. al. 2023) **This work**

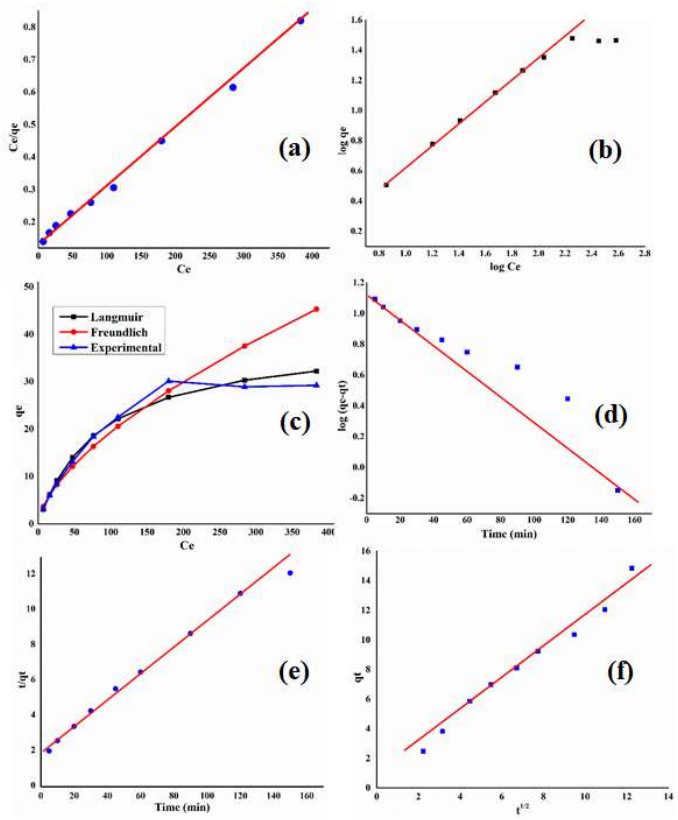

IV. Conclusion

A microporous crosslinked Cs–Ac composite was successfully synthesized and then analyzed by various characterizations. The composite was utilized to remove Reactive Orange 16 dye (anionic dye) from aqueous medium. Cs–Ac was characterized using various techniques, which confirmed the formation of a composite having STPP crosslinked well to the chitosan. SEM micrographs and EDAX analysis showed the morphological transformation and composition of Cs–Ac, respectively. BET surface area analysis using the nitrogen adsorption–desorption method revealed a good surface area and pore volume and also confirmed the microporous nature of the adsorbent. The amount of dye adsorption was dependent on the adsorbent dosage, temperature, and contact time. The maximum q_t of Cs–Ac was obtained from the Langmuir model as 39.43 mg g^{-1}, which was quite high compared to most existing biosorbents. The thermodynamics results indicated that the adsorption process was spontaneous and endothermic in nature and was entropy driven. The adsorption mechanism of the Reactive Orange 16 dye on the Cs–Ac surface could be assigned to various types of interactions, such as electrostatic attraction, H-bonding interaction, and π-π interaction. The adsorption results indicated that Cs–Ac can be considered as a feasible and promising biosorbent for the removal of anionic dyes from an aqueous environment. A comparison with the reported materials, as shown in Table 2, highlights the advantage of this material over the previously reported materials for the adsorption of Reactive Orange 16 dye.

V. References

Ahmed, M. J.; Okoye, P. U.; Hummadi, E. H. and Hameed, B. H. (2019). High-performance porous biochar from the pyrolysis of natural and renewable seaweed (Gelidiella acerosa) and its application for the adsorption of methylene blue. Bioresour. Technol. 278, 159–164.

Ahmed, S. and Iqbal, A. (2018). Synthesis of 2D magnesium oxide nanosheets: a potential material for phosphate removal. Global Challenges. 2, 1800056.

Al-Degs, Y.; Khraisheh, M. A. M.; Allen, S. J. and Ahmad, M. N. (2000). Effect of carbon surface chemistry on the removal of reactive dyes from textile effluent. Water Res. 34, 927–935.

Ali, I.; Alharbi, O. M. L.; Alothman, Z. A.; Al-Mohaimeed, A. and Alwarthan, A. (2019). Modeling of fenuron pesticide adsorption on CNTs for mechanistic insight and removal in water. Environ. Res. 170, 389–397.

Alothman, Z. A.; Bahkali, A.; Khiyami, M.; Alfadul, S.; Wabaidur, S.; Alam, M. and Alfarhan, B. (2020). Low cost biosorbents from fungi for heavy metals removal from wastewater. Sep. Sci. Technol. 55, 1766–1775.

Behera, M.; Nayak, J.; Banerjee, S.; Chakrabortty, S. and Tripathy, S. K. (2021). A review on the treatment of textile industry waste effluents towards the development of efficient mitigation strategy: An integrated system design approach. J. Environ. Chem. Eng. 9, 105277.

Bhumkar, D. R. and Pokharkar, V. B. (2006). Studies on effect of pH on cross-linking of chitosan with sodium tripolyphosphate: a technical note. AAPS Pharm. Sci. Tech. 7, E138–E143.

Butt, M. T.; Imtiaz, N.; Ahmed, S.; Arif, F. and Khan, S. R. (2010). Colour Removal from Textile Dyeing Wastewater Using Different Adsorbents. Pak. J. Sci. Ind. Res., Ser. B. 53, 81–84.

Cunico, P.; Kumar, A. and Fungaro, D. A. (2015). Adsorption of dyes from simulated textile wastewater onto modified nanozeolite from coal fly ash. Journal of Nanoscience and Nanoengineering, 1(3), 148-161.

Dwyer, J.; Griffiths, P. and Lant, P. (2009). Simultaneous colour and DON removal from sewage treatment plant effluent: Alum coagulation of melanoidin. Water Res. 43, 553–561.

Elsabee, M. Z.; Morsi, R. E. and Al-Sabagh, A. M. (2009). Surface active properties of chitosan and its derivatives. Colloids Surf. B. 74, 1–16.

Faysal Hossain, M. D.; Akther, N. and Zhou, Y. (2020). Recent advancements in graphene adsorbents for wastewater treatment: Current status and challenges. Chin. Chem. Lett. 31, 2525–2538.

Freundlich, H. M. (1906). Over the Adsorption in Solution. Phys. Chem. 57, 385–470.

Guo, M.; Wang, J.; Wang, C.; Strong, P. J.; Jiang, P.; Ok, Y. S. and Wang, H. (2019). Carbon nanotube-grafted chitosan and its adsorption capacity for phenol in aqueous solution. Sci. Total Environ. 682, 340–347.

Jawad, A. H.; Abdulhameed, A. S. and Mastuli, M. S. (2020). Mesoporous crosslinked chitosan-activated charcoal composite for the removal of thionine cationic dye: comprehensive adsorption and mechanism study. J. Polym. Environ. 28, 1095–1105.

Jesus, A. M. D.; Romão, L. P. C.; Araújo, B. R.; Costa, A. S. and Marques, J. J. (2011). Use of humin as an alternative material for adsorption/desorption of reactive dyes. Desalination, 274(1-3), 13-21.

Kahu, S.; Shekhawat, A.; Saravanan, D. and Jugade, R. (2016). Ionic solid-impregnated sulphate-crosslinked chitosan for effective adsorption of hexavalent chromium from effluents. Int. J. Environ. Sci. Technol. 13, 2269–2282.

Kenawy, E. R.; Ghfar, A. A.; Wabaidur, S. M.; Khan, M. A. ; Siddiqui, M. R. and Alothman, Z. A. (2018). Cetyltrimethylammonium bromide intercalated and branched polyhydroxystyrene functionalized montmorillonite clay to sequester cationic dyes. J. Environ. Manage. 219, 285–293.

Khan, M.; Alqadami, A.; Wabaidur, S.; Siddiqui, M.; Jeon, B.; Alshareef, S.; Alothman, Z. and Hamedelniel, A. (2020). Oil industry waste based non-magnetic and magnetic hydrochar to sequester potentially toxic post-transition metal ions from water. J. Hazard. Mater. 400, 123247.

Khan, T.; Nouman, M.; Dua, D.; Khan, S. and Alharthi, S. (2022). Adsorptive scavenging of cationic dyes from aquatic phase by H3PO4 activated Indian jujube (Ziziphus mauritiana) seeds based activated carbon: Isotherm, kinetics, and thermodynamic study. J. Saudi Chem. Soc. 26, 101417.

Khapre, M. A.; Pandey, S. and Jugade, R. M. (2021). Glutaraldehyde-cross-linked chitosan–alginate composite for organic dyes removal from aqueous solutions. Int. J. Biol. Macromol. 190, 862–875.

Korde, S.; Deshmukh, S.; Tandekar, S. and Jugade, R. (2021). Implementation of response surface methodology in physi-chemisorption of Indigo carmine dye using modified chitosan composite. Carbohydr. Polym. Technol. Appl. 2, 100081.

Korde, S.; Tandekar, S.; Saravanan, D. and Jugade, R. (2020). Novel mesoporous chitosan-zirconia-ferrosoferric oxide as magnetic composite for defluoridation of water. J. Environ. Chem. Eng. 8, 104360.

Langmuir, I. (1918). The adsorption of gases on plane surfaces of glass, mica and platinum. J. Am. Chem. Soc. 40, 1361–1403.

Leal, G. F.; Ramos, L. A.; Barrett, D. H.; Curvelo, A. A. S. and Rodella, C. B. (2015). Thermogravimetric analysis (TGA) method to determine the catalytic conversion of cellulose from carbon-supported hydrogenolysis process. Thermochim. Acta. 616, 9–13.

Lee, C. K.; Ong, S. T. and Zainal, Z. (2008). Ethylenediamine modified rice hull as a sorbent for the removal of Basic Blue 3 and Reactive Orange 16. International Journal of Environment and Pollution, 34(1-4), 246-260.

Li, Z.; Go´mez-Avile´s, A.; Sellaoui, L.; Bedia, J.; BonillaPetriciolet, A. and Belver, C. (2019). Adsorption of ibuprofen on organo-sepiolite and on zeolite/sepiolite heterostructure: Synthesis, characterization and statistical physics modeling. Chem. Eng. J. 371, 868–875.

Nandanwar, P.; Jugade, R.; Gomase, V.; Shekhawat, A.; Bambal, A.; Saravanan, D. and Pandey, S. (2023). Chitosan-biopolymer-entrapped activated charcoal for adsorption of reactive orange dye from aqueous phase and CO_2 from gaseous phase. Journal of Composites Science, 7(3), 103.

Naushad, M.; Sharma, G. and Alothman, Z. A. (2019). Photodegradation of toxic dye using Gum Arabic-crosslinked-poly(acrylamide)/Ni(OH)2/FeOOH nanocomposites hydrogel. J. Cleaner Prod. 241, 118263.

Ozturk, G. and Silah, H. (2020). Adsorptive Removal of Remazol Brilliant Blue R from water by using a macroporous polystyrene resin: Isotherm and kinetic studies. Environ. Processes. 7, 479–492.

Pala, A. and Tokat, E. (2002). Color removal from cotton textile industry wastewater in an activated sludge system with various additives. Water Res. 36, 2920–2925.

Qi, X.; Chen, M.; Qian, Y.; Liu, M.; Li, Z.; Shen, L.; Qin, T.; Zhao, S.; Zeng, Q. and Shen, J. (2019). Construction of macroporous salecan polysaccharide-based adsorbents for wastewater remediation. Int. J. Biol. Macromol. 132, 429–438.

Qi, X.; Lin, L.; Shen, L.; Li, Z.; Qin, T.; Qian, Y.; Wu, X.; Wei, X.; Gong, Q. and Shen, J. (2019). Efficient decontamination of lead ions from wastewater by salecan polysaccharide-based hydrogels. ACS Sustainable Chem. Eng. 7, 11014–11023.

Robinson, T.; McMullan, G.; Marchant, R. and Nigam, P. (2001). Remediation of dyes in textile effluent: a critical review on current treatment technologies with a proposed alternative. Bioresour. Technol. 77, 247–255.

Rojas, S. and Horcajada, P. (2020). Metal–Organic Frameworks for the Removal of Emerging Organic Contaminants in Water. Chem. Rev., 120, 8378–8415.

Royer, B.; Cardoso, N. F.; Lima, E. C.; Ruiz, V. S.; Macedo, T. R. and Airoldi, C. (2009). Organofunctionalized kenyaite for dye removal from aqueous solution. Journal of Colloid and Interface Science, 336(2), 398-405.

San Miguel, G.; Lambert, S. D. and Graham, N. J. D. (2006). A practical review of the performance of organic and inorganic adsorbents for the treatment of contaminated waters. J. Chem. Technol. Biotechnol., 81, 1685–1696.

Subbaiah, M. V. and Kim, D.-S. (2016). Adsorption of methyl orange from aqueous solution by aminated pumpkin seed powder: Kinetics, isotherms, and thermodynamic studies. Ecotoxicol. Environ. Saf. 128, 109–117.

Sun, Z.; Duan, X.; Srinivasakannan, C. and Liang, J. (2018). Correction: Preparation of magnesium silicate/carbon composite for adsorption of rhodamine B. RSC Adv. 8(16), 8625.

Tandekar, S.; Korde, S. and Jugade, R. (2021). Red mud-chitosan microspheres for removal of coexistent anions of environmental significance from water bodies. Carbohydr. Polym. Technol. Appl. 2, 100128.

Tang, H.; Zhou, W. and Zhang, L. (2012). Adsorption isotherms and kinetics studies of malachite green on chitin hydrogels. J. Hazard. Mater. 209–210, 218–225.

Theerakarunwong, C. and Boontong, D. (2020). Removal and recyclable chitosan nanowires: Application to water soluble dyes. Results Chem. 2, 100024.

Wabaidur, S. M.; Khan, M.; Siddiqui, M.; Otero, M.; Jeon, B.; Alothman, Z. and Hakami, A. (2020). Oxygenated functionalities enriched MWCNTs decorated with silica coated spinel ferrite–A nanocomposite for potentially rapid and efficient de-colorization of aquatic environment. J. Mol. Liq. 317, 113916.

Yang, F.; Sheng, B.; Wang, Z.; Xue, Y.; Liu, J.; Ma, T.; Bush, R., Kusˇic´ H. and Zhou, Y. (2021). Performance of UV/acetylacetone process for saline dye wastewater treatment: Kinetics and mechanism. J. Hazard. Mater. 406, 124774.

Yang, J.; Han, Y.; Sun, Z.; Zhao, X.; Chen, F.; Wu, T. and Jiang, Y. (2021). PEG/Sodium Tripolyphosphate-Modified Chitosan/Activated Carbon Membrane for Rhodamine B Removal. ACS Omega. 6, 15885–15891.

Zhou, Y.; Lu, J.; Zhou, Y. and Liu, Y. (2019). Recent advances for dyes removal using novel adsorbents: a review. Environ. Pollut. 252, 352–365.